Author(s): Dias, Cristiano L. & Ala-Nissilä, Tapio & Karttunen, Mikko & Vattulainen, Ilpo & Grant, Martin

Title: Microscopic Mechanism for Cold Denaturation

Year: 2008

Version: Final published version

Please cite the original version:

Dias, Cristiano L. & Ala-Nissilä, Tapio & Karttunen, Mikko & Vattulainen, Ilpo & Grant, Martin. 2008. Microscopic Mechanism for Cold Denaturation. Physical Review Letters. Volume 100, Issue 11. P. 118101/1-4. ISSN 0031-9007 (printed). DOI: 10.1103/physrevlett.100.118101.

Microscopic Mechanism for Cold Denaturation

Cristiano L. Dias,[1] Tapio Ala-Nissila,[2,3] Mikko Karttunen,[4] Ilpo Vattulainen,[5,6,7] and Martin Grant[1]

[1]*Physics Department, Rutherford Building, McGill University, 3600 rue University, Montréal, Québec, Canada H3A 2T8*
[2]*Department of Physics, Brown University, Providence, Rhode Island 02912-1843, USA*
[3]*Department of Engineering Physics, Helsinki University of Technology, P.O. Box 1100, FI-02015 TKK, Espoo, Finland*
[4]*Department of Applied Mathematics, The University of Western Ontario, London, Ontario, Canada*
[5]*Institute of Physics, Tampere University of Technology, P.O. Box 692, FI-33101 Tampere, Finland*
[6]*MEMPHYS–Center for Biomembrane Physics, University of Southern Denmark, Odense, Denmark*
[7]*Helsinki Institute of Physics, Helsinki University of Technology, Helsinki, Finland*

(Received 20 April 2007; published 18 March 2008)

We elucidate the mechanism of cold denaturation through constant-pressure simulations for a model of hydrophobic molecules in an explicit solvent. We find that the temperature dependence of the hydrophobic effect induces, facilitates, and is the driving force for cold denaturation. The physical mechanism underlying this phenomenon is identified as the destabilization of hydrophobic contact in favor of solvent-separated configurations, the same mechanism seen in pressure-induced denaturation. A phenomenological explanation proposed for the mechanism is suggested as being responsible for cold denaturation in real proteins.

DOI: 10.1103/PhysRevLett.100.118101 PACS numbers: 87.14.E−, 87.15.−v, 87.15.A−, 87.15.B−

Under physiological conditions, proteins adopt a unique three-dimensional (3D) structure [1]. This structure is maximally stable at about 17 °C and becomes unstable at both high (∼ 60 °C) and low (−20 °C) temperatures [2–4]. The latter phenomenon, where the protein unfolds thereby increasing its entropy, is called cold denaturation and is accompanied by a decrease in the entropy of the entire system. This counterintuitive behavior has been experimentally verified [3,5] but has remained a subject of controversy [2,4], since a satisfactory microscopic explanation for this phenomenon has not yet emerged. Resolving cold denaturation microscopically would facilitate understanding the forces responsible for the structure of proteins and, in particular, the role of the complex hydrophobic effect.

In the case of diluted proteins, hydrophobicity is considered the main driving force for folding and unfolding [6]. Consequently, cold denaturation has been studied using explicit models that take hydrophobicity into account [7–10]. One class of such models [7,9] associates the phenomena with the different energetic states of shell water, i.e., water molecules neighboring the protein, in a lattice. A more realistic water model [8] supports this view, as water-water hydrogen bonding among shell water has been found to increase at low temperatures and to correlate with cold denaturation. Meanwhile, another class of models suggests that the density fluctuations of water are responsible for cold denaturation [11,12]. Despite the lack of consensus in the explanation of cold denaturation, the solvent is widely accepted as the key player. This is also supported by the fact that denaturation also takes place under pressure [13,14]. By focusing on the transfer of water molecules to the protein interior, pressure denaturation has been explained through the destabilization of hydrophobic contacts in favor of solvent-separated configurations [13]. This destabilization has been verified using different water models [15].

In the present work, we examine the microscopic physical mechanism behind cold denaturation. To this end, we consider the two-dimensional Mercedes-Benz (MB) model to describe water molecules in the solvent and a simple bead-spring model for the protein. The MB model reproduces many of the properties of water [16], including the temperature dependent behavior of the hydrophobic effect [17]. Our simulations provide a simple microscopic picture for cold denaturation in terms of changes in hydration: at low temperatures water molecules infiltrate the folded protein in order to passivate the ''dangling'' water-water hydrogen bonds (H bonds) found in shell water. At the same time, hydrophobic contacts are destabilized and an ordered layer of water molecules forms around the protein monomers such that they become separated by a layer of solvent in the cold denatured state. Hence, increasing pressure and decreasing temperature destabilize hydrophobic contacts in favor of similar solvent-separated configurations. We expect that this aggravated destabilization of hydrophobic contacts at high pressure explains why the transition temperature for cold denaturation increases with increasing pressure [2]. Here, we study cold denaturation at the equivalent of ambient pressure.

As in water, the interaction between the MB molecules is given by a sum of hydrogen bonds and van der Waals bonds. The directionality of H bonds is accounted for by three arms separated by an angle of 120°. This interaction has maximal strength when arms of neighboring molecules are aligned. If $\vec{r}_{ij}$ is the distance vector between the center of mass of molecules i and j, and $\vec{r}_{i\alpha}$ is the distance vector between the center of molecule i and the extremity of arm α, then the interaction energy is given by

$$V_{\mathrm{H}}(\vec{r}_{ij},\{\vec{r}_{i\alpha}\},\{\vec{r}_{j\beta}\}) = \epsilon_{\mathrm{H}}\exp\left(-\frac{(r_{ij}-R_{\mathrm{H}})^2}{2\sigma_R^2}\right) \times\left\{\sum_{\alpha=1}^{3}\exp\left[-\left(\frac{\vec{r}_{i\alpha}\cdot\vec{r}_{ij}}{r_{ij}r_{i\alpha}}-1\right)^2\frac{1}{2\sigma_\theta^2}\right]\right\} \times\left\{\sum_{\beta=1}^{3}\exp\left[-\left(\frac{\vec{r}_{j\beta}\cdot\vec{r}_{ij}}{r_{ij}r_{j\beta}}-1\right)^2\frac{1}{2\sigma_\theta^2}\right]\right\}, \quad (1)$$

where ϵ_{H} and R_{H} are the binding energy and the equilibrium (reference) length of the bond, respectively. The constants σ_R and σ_θ are attenuation parameters of the interaction. Equation (1) favors configurations where the distance between molecules i and j is R_{H}, one arm of molecule i is aligned with the line joining the two centers of mass, and the same for one arm of molecule j. The van der Waals interaction is described by a Lennard-Jones (LJ) potential V_{ww} with binding energy ϵ_{ww} and equilibrium length R_{ww}:

$$V_{ww}(r_{ij}) = 4\epsilon_{ww}\left[\left(\frac{R_{ww}}{r_{ij}}\right)^{12}-\left(\frac{R_{ww}}{r_{ij}}\right)^{6}\right]. \quad (2)$$

The LJ potentials are shifted so that the force becomes zero at the cutoff distance $R_c = 2.5R_{\mathrm{H}}$ [18]. We use the parameter set that has been studied extensively by Silverstein *et al.* [16]: $\epsilon_{\mathrm{H}} = 1.0$, $R_{\mathrm{H}} = 1.0$, $\sigma_R = \sigma_\theta = 0.085$, $\epsilon_{ww} = 0.1$, and $R_{ww} = 0.7$. The total interaction energy $V_{i,j}$ between two water molecules is given by the sum of Eqs. (1) and (2).

Here, we set $M_w = 1$ for water. To mimic the distribution of mass in water, $1/10$ of the total mass of a water molecule is located at each arm's extremity and the extremity of an arm is located at a distance $R_{\mathrm{arm}} = 0.36R_{\mathrm{H}}$ from the center of mass [19]. This defines the angular momentum of the water molecule.

Energies, distances, and time are given in units of ϵ_{H}, R_{H}, and $\tau_o = \sqrt{\epsilon_{ww}/M_w R_{ww}^2}$, respectively. To model the protein, we use a bead-spring model: monomers that are adjacent along the backbone of the protein are connected to each other by springs, and nonadjacent monomers are connected by a shifted LJ potential. The LJ potential is described by a binding energy $\epsilon_{\mathrm{mm}} = 0.375$ and distance R_{mm}. The equilibrium length and stiffness of the spring are R_{spring} and $K_{\mathrm{spring}} = 2(456\epsilon_{\mathrm{mm}}/R_{\mathrm{mm}}^2)$. This corresponds to twice the stiffness of the LJ potential. Monomers are set to be 10 times heavier than water molecules. The interaction between monomers and water molecules is given by a shifted LJ potential with binding energy $\epsilon_{\mathrm{wm}} = \epsilon_{ww}$ and equilibrium length R_{wm}.

When the side chain of a hydrophobic amino acid is exposed to the solvent, the liquid surrounding the side chain assumes a cagelike configuration [20] in order to minimize the amount of broken H bonds of water molecules. This configuration has a low entropy and proteins minimize their free energy by burying these hydrophobic amino acids in their interior. To reproduce this, we choose $R_{\mathrm{spring}} = 2.0$ and $R_{\mathrm{wm}} = 0.9$ such that monomers can be surrounded by a layer of water molecules when exposed to the solvent. To allow for the formation of a dry protein core, we use $R_{\mathrm{mm}} \backsimeq R_{\mathrm{wm}}$, though $2R_{\mathrm{mm}} > R_{\mathrm{spring}}$ to avoid the backbone from intersecting itself. Taking these restrictions into account, we choose $R_{\mathrm{mm}} = 1.1$.

Having defined the interaction between the different particles, we now perform molecular dynamics in the isothermal-isobaric ensemble. Constant pressure is achieved using Andersen extended method [21] implemented using the simplectic algorithm [22]. For the mass Q and the friction constant γ_V of the piston acting on the simulation box, we use $Q = 0.054/R_{ww}^4$ and $\gamma_V = 0.5$. A parallelogram with equal sides and defined by an angle of 120° is used for the simulation box. This geometry retains the periodicity of a crystal made of water molecules through the boundaries. For the Langevin equations describing the motion of particles, we use the friction constant $\gamma^{-1} = 0.93\tau_o$. The noise term in the Langevin equations of motion is given by the fluctuation-dissipation theorem. Pressure is set to 0.2 in units of $\epsilon_{\mathrm{H}}/R_{\mathrm{H}}^2$. At this pressure, the MB model reproduces waterlike anomalies seen at ambient pressure [17] and hydrates nonpolar molecules in a realistic manner [23]. The simulation box is composed of a 10-monomer long protein and 502 water molecules. To represent the solvent in its liquid state, we use temperatures ranging from 0.145 to 0.25 in units of ϵ_{H} [24].

The system was initially equilibrated at a temperature of 0.25 for 5000 time steps, followed by a data collection period of 50 000 time steps. The temperature was then lowered and the equilibration-collection cycle was repeated. This cooling procedure was repeated until the lowest temperature was reached. Four samples with different initial conditions were prepared using this protocol, and the distribution of the protein's radius of gyration R_G [25] was computed. To obtain equilibrium properties, the final configuration at each temperature was used to extend the simulation time until the distribution of R_G of the four samples converged within a root-mean-square value of 0.02.

In Fig. 1, we show the equilibrium distribution of R_G averaged over the four samples at three different temperatures. An initial decrease in temperature, from 0.25 to 0.21, shifts the peak of the distribution to a lower value. Therefore, in *hot water*, proteins favor more compact configurations when the temperature of the system is lowered. However, a further decrease of temperature results in completely different behavior: as the temperature decreases from 0.21 to 0.17, the peak shifts to a larger value indicating that in *cold water* proteins become less compact for decreasing temperature. This behavior in hot and cold water is shown systematically in the inset of Fig. 1, which depicts the temperature dependence of R_G. The radius of

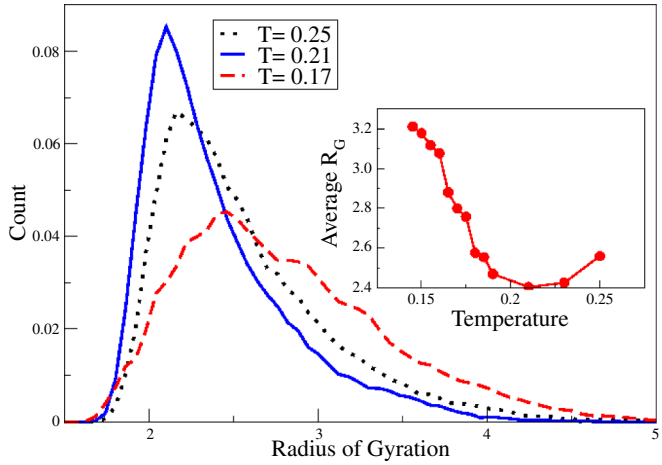

FIG. 1 (color online). Normalized distribution of the radius of gyration R_G at three temperatures: $T = 0.25$, $T = 0.21$, and $T = 0.17$. Inset: The temperature dependence of R_G of the protein.

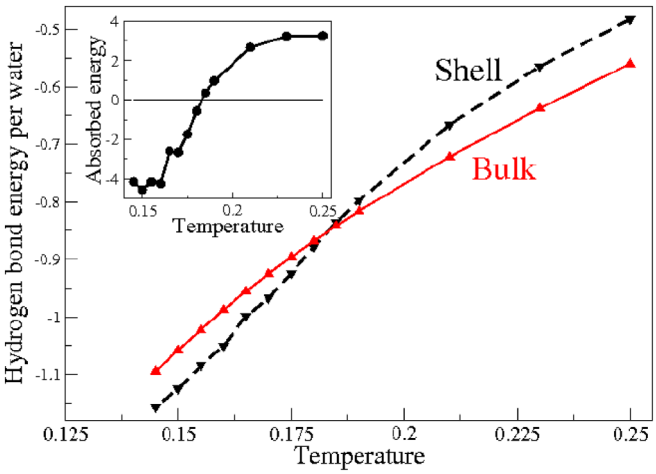

FIG. 2 (color online). Hydrogen bond energy per water molecule for shell and bulk water. Inset: Absorbed energy to accommodate the protein at different temperatures. The shell is defined by water molecules whose distance to the protein is less than 2.5 in units of R_H.

gyration decreases as temperature decreases towards 0.21. Below that temperature, R_G increases monotonically as temperature decreases. These two types of behavior are characteristic of heat and cold denaturation of real proteins and are in line with previous studies [2,8,9].

The paraboliclike shape of R_G (see the inset of Fig. 1) cannot be mapped into a model with local monomer-monomer interactions only [7]. To study the role of water, we show in Fig. 2 the average H bond energy per water molecule for shell and bulk water. The energy of shell water averaged over the different configurations is higher than the energy of bulk water at high temperatures. This changes gradually as temperature decreases such that the creation of shell water becomes energetically favorable at low temperatures. Therefore, when a protein is immersed in cold water, it releases heat to form the shell, while in hot water it absorbs heat. These features are again characteristic of cold and heat denaturation of real proteins [4]. In the inset of Fig. 2 we show the energy absorbed by the system to create the shell around the protein. The absorbed energy is defined as the difference in H bond energy between shell and bulk water multiplied by the average number of molecules forming the shell. The absorbed energy decreases monotonically with decreasing temperature and becomes negative below some T indicating heat release.

Characteristic configurations of the protein at different temperatures are shown in Fig. 3. In cold water (upper panels), the solvent forms a cage around each monomer of the protein; i.e., monomers are surrounded by an ordered layer of water molecules. Molecules forming the cage are strongly H bonded to each other and therefore have a low energy. At $T = 0.21$, the protein favors compact configurations. Water molecules close to the protein have at least one nonsaturated H bond, which is pointing towards the protein. When the temperature is increased to $T = 0.25$, most monomers are in contact with the solvent. The solvent forms incomplete cages around monomers, i.e., cages that do not surround monomers from all sides, or they correspond to particles that are weakly bonded to the other solvent particles and are thus energetic. The crossover behavior of shell water shown in Fig. 2 is therefore characterized by the formation of cagelike configurations at low temperatures and the presence of dangling H bonds at high temperatures [26].

Configurations where monomers are separated by an ordered layer of solvent molecules have also been shown

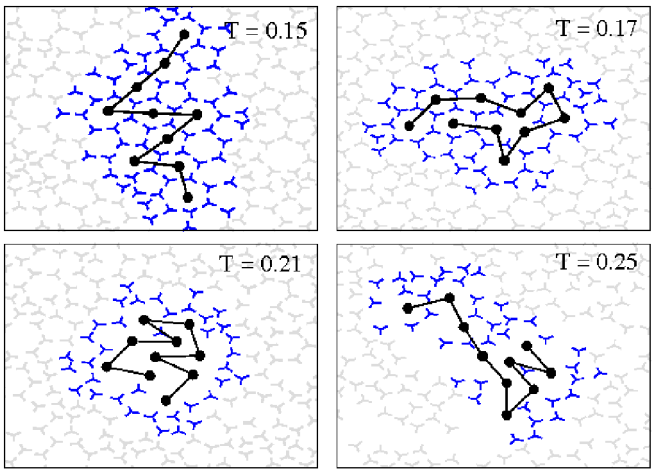

FIG. 3 (color online). Characteristic configurations of a protein in cold water ($T = 0.15$ and $T = 0.17$), at an intermediate temperature ($T = 0.21$), and in hot water ($T = 0.25$). The distance of highlighted (shell) water molecules to the protein is less than 2.5 in units of R_H. In cold water, the monomers are typically surrounded by clathratelike cages.

to become more stable, as temperature decreases, in models for the hydrophobic effect of methanelike solutes [23,27]. Solvent layers around those monomer pairs are highly ordered such that their formation decreases the entropy of the system. Unfolding at low temperatures is therefore accompanied by a lowering in the entropy of the *total* system in accordance with experiments [4], shell water molecules becoming more ordered as the protein becomes less ordered. This mechanism explains the counterintuitive decrease in entropy during cold denaturation. The phenomenology is as follows. When nonpolar solutes are transferred into water, the system relaxes by ordering those solvent molecules around the solute. This ordering has an entropic cost, which is minimized by clustering nonpolar solutes together, as this decreases the amount of surface around solutes. As the temperature decreases below a particular value, the system rebuilds the ordered layer of solvent around nonpolar solutes to saturate the dangling H bonds left on the surface of clustered solutes—minimizing the enthalpy. This behavior should also be valid close to crystallization where both shell and bulk water are about to freeze and therefore have similar entropies. In this situation the free energy is mostly minimized through enthalpy and the system favors ordered layers of solvent molecules. Although hydrophobicity is not the only force responsible for the stability of proteins, the formation of a hydrophobic core plays the dominant role.

In conclusion, we find that, at low temperatures, shell water forms hydrogen bonds better than bulk water. Microscopically this correlates with the presence of solvent-separated configurations, which accounts for the unfolding of the protein at low temperatures. The existence of such low energetic states for shell water at low T explains why cold denaturation proceeds with heat release as opposed to heat absorption seen during heat denaturation. Although here we studied cold denaturation in two dimensions, solvent-separated configurations have also been shown to become more favorable as temperature decreases in a 3D model for the hydrophobic effect [27]. Therefore we expect that the results found in this work remain valid in 3D systems. Our results further suggest that cold and pressure denaturation could be studied under a single framework: a transition towards solvent-separated-configurations [13].

This work was supported by the Natural Sciences and Engineering Research Council of Canada, and *le Fonds Québécois de la recherche sur la nature et les technologies*. I. V. and T. A-N. thank the Academy of Finland through its COMP Center of Excellence and TransPoly grants.

[1] C. B. Anfinsen, Science **181**, 223 (1973).
[2] S. Kunugi and N. Tanaka, Biochim. Biophys. Acta **1595**, 329 (2002); L. Smeller, Biochim. Biophys. Acta **1595**, 11 (2002).
[3] P. L. Privalov, J. Chem. Thermodyn. **29**, 447 (1997).
[4] P. L. Privalov, Y. V. Griko, and S. Y. Venyaminov, J. Mol. Biol. **190**, 487 (1986).
[5] R. Ravindra and R. Winter, Chem. Phys. Chem. **4**, 359 (2003).
[6] K. A. Dill, Biochemistry **29**, 7133 (1990); W. Kauzmann, Adv. Protein Chem. **14**, 1 (1959); H. Li, C. Tang, and N. S. Wingreen, Phys. Rev. Lett. **79**, 765 (1997).
[7] P. Bruscolini and L. Casetti, Phys. Rev. E **61**, R2208 (2000).
[8] D. Paschek, S. Nonn, and A. Geiger, Phys. Chem. Chem. Phys. **7**, 2780 (2005).
[9] P. D. L. Rios and G. Caldarelli, Phys. Rev. E **62**, 8449 (2000); P. D. L. Rios and G. Caldarelli, Phys. Rev. E **63**, 031802 (2001).
[10] O. Collet, Europhys. Lett. **53**, 93 (2001).
[11] M. I. Marques, J. M. Borreguero, H. E. Stanley, and N. V. Dokholyan, Phys. Rev. Lett. **91**, 138103 (2003).
[12] S. V. Buldyrev, P. Kumar, and H. E. Stanley, arXiv:cond-mat0701485.
[13] G. Hummer, S. Garde, A. E. Garcia, and M. E. Paulaitis, Proc. Natl. Acad. Sci. U.S.A. **95**, 1552 (1998).
[14] F. Meersman, C. M. Dobson, and K. Heremans, Chem. Soc. Rev. **35**, 908 (2006).
[15] T. Ghosh, A. E. García, and S. Garde, J. Am. Chem. Soc. **123**, 10997 (2001).
[16] K. A. T. Silverstein, A. D. J. Haymet, and K. A. Dill, J. Am. Chem. Soc. **120**, 3166 (1998).
[17] K. A. Dill, T. M. Truskett, V. Vlachy, and B. Hribar-Lee, Annu. Rev. Biophys. Biomol. Struct. **34**, 173 (2005).
[18] M. P. Allen and D. J. Tildesley, *Computer Simulations of Liquids* (Clarendon, Oxford, 1990).
[19] A. Rahman and F. H. Stillinger, J. Chem. Phys. **55**, 3336 (1971).
[20] D. T. Bowron, A. Filipponi, M. A. Roberts, and J. L. Finney, Phys. Rev. Lett. **81**, 4164 (1998).
[21] H. C. Andersen, J. Chem. Phys. **72**, 2384 (1980).
[22] A. Kolb and B. Dünweg, J. Chem. Phys. **111**, 4453 (1999).
[23] N. T. Southall and K. A. Dill, Biophys. Chem. **101–102**, 295 (2002).
[24] Although the solidification temperature for a system containing 60 MB particles was found to be 0.16 [16], this temperature scales with the size of the system—see, for example, J. Lee and J. M. Kosterlitz, Phys. Rev. B **43**, 3265 (1991). For the system studied here the peak in the specific heat, which defines the transition temperature, is found at a temperature of 0.145.
[25] M. Doi and S. F. Edwards, *The Theory of Polymer Dynamics* (Oxford University Press, New York, 1988).
[26] See EPAPS Document No. E-PRLTAO-100-052809 for additional evidence for the high occurrence of cagelike configurations at low temperature. For more information on EPAPS, see http://www.aip.org/pubservs/epaps.html.
[27] D. Paschek, J. Chem. Phys. **120**, 6674 (2004); S. Shimizu and H. S. Chan, J. Chem. Phys. **113**, 4683 (2000); T. Ghosh, A. E. García, and S. Garde, J. Chem. Phys. **116**, 2480 (2002).